

Generation of upstream waves by a moving pressure distribution with dynamic correction at near-critical speed

Jinyu Yao^{1*}, Harry B. Bingham², Xinshu Zhang¹

¹State Key Laboratory of Ocean Engineering, Shanghai Jiao Tong University, Shanghai 200240, China

²Department of Civil & Mechanical Engineering, Technical University of Denmark, Lyngby, Denmark

1 Introduction

The type of waves generated by a ship in steady motion over a flat bottom varies with the depth Froude number $Fr = U/\sqrt{gh}$ (where g is the acceleration of gravity and h is the water depth). In the sub-critical condition ($Fr < 1$), a wake wave and a depression along the ship are formed. In the critical ($Fr = 1$) and supercritical ($Fr > 1$) conditions, upstream nonlinear solitons are generated at the bow. Boussinesq equations were adopted by Wu & Wu (1982) to simulate a two-dimensional pressure patch moving on the free surface at a near-critical speed ($Fr \sim 1$). It was found that upstream solitons are generated periodically. Based on a series of experiments in a channel with restricted width, Ertekin *et al.* (1984) found the crestline of upstream solitons is straight and solitons begin to break at $Fr = 1.2$. Ertekin *et al.* (1986) used Green-Naghdi equations to model the propagation of solitons generated by a three-dimensional disturbance. It was found that periodic generation of solitons induces periodic oscillation of the wave drag. Based on a modified generalized Boussinesq equation, Li & Scavounos (2002) investigated three-dimensional solitons generated by a ship traveling in horizontally unbounded water. Solitons which propagate in an unbounded domain have a parabolic crestline and do not break at $Fr = 1.2$. Shi *et al.* (2018) used a fully nonlinear Boussinesq model combined with a viscosity dissipation scheme and a shock-capturing dissipation scheme, and investigated the transition from breaking solitons to a pure bore. Based on the forced Korteweg-de Vries equation, Wu (1987) explained the mechanism of the formation of upstream solitons and found that their generation can be attributed to a well-balanced interplay between nonlinearity and dispersion in the wave. By comparing the waves induced by a high pressure system and a low pressure system, Grue (2022) illustrated the dispersive effect of the upstream generation of three-dimensional solitons at $Fr = 1$.

In near-critical conditions ($Fr \sim 1$), ship-generated upstream waves are nonlinear phenomena which cannot be captured by a linear model and have been widely simulated by nonlinear models based on Boussinesq or Korteweg-de Vries equations, e.g. Li & Scavounos (2002) and Wu (1987). In this paper, we use a high-order spectral (HOS) method to model the generation and propagation of upstream waves. A moving pressure distribution is adopted to model the traveling ship; however, in contrast to most previous work where a static pressure models the ship, such as Shi *et al.* (2018), we use a dynamic correction strategy to simulate a travelling ship. The upstream waves in test cases with various Fr around 1 and different water depths h are studied. To validate our numerical results, experimental records in Ertekin *et al.* (1984) are provided for comparison.

2 High-order spectral model

The high-order spectral model, which was initially proposed by Dommermuth & Yue (1987) and West *et al.* (1987), is based on the potential flow formalism. The fluid is assumed to be homogeneous, inviscid, incompressible, and the fluid motion is irrotational. The fluid domain is three-dimensional. x and y are the two horizontal axes, and z is the vertical axis pointing upwards. The flow is described by a velocity potential $\phi(x, y, z)$, which satisfies the Laplace equation:

$$\Delta\phi = 0. \quad (1)$$

The surface potential is described by $\phi^S(x, y, z, t) = \phi(x, y, \eta(x, y, t), t)$ where η is the free surface elevation, then the nonlinear free-surface boundary conditions are

$$\eta_t + \nabla\phi^S \cdot \nabla\eta - \phi_z(1 + \nabla\eta \cdot \nabla\eta) = 0, \quad \text{at } z = \eta, \quad (2)$$

$$\phi_t^S + g\eta + \frac{1}{2}\nabla\phi^S \cdot \nabla\phi^S - \frac{1}{2}\phi_z^2(1 + \nabla\eta \cdot \nabla\eta) = -\frac{p}{\rho}, \quad \text{at } z = \eta, \quad (3)$$

*Presenting author

where $\nabla_1 = (\frac{\partial}{\partial x}, \frac{\partial}{\partial y})$, ρ , g and p are the water density, gravitational acceleration and ship pressure distribution, respectively. A flat bottom is assumed and the water depth is h . The bottom boundary condition reads

$$\phi_z(x, y, z) = 0, \quad \text{at } z = -h. \quad (4)$$

Periodic boundary conditions are used in the horizontal plane. The potential is expressed by a truncated power series, i.e. $\phi = \sum_{m=1}^M \phi^{(m)}$. To satisfy the Laplace equation and the boundary conditions in the fluid domain, $\phi^{(m)}$ is written as

$$\phi^{(m)} = \sum_p \sum_q A_{pq}^{(m)}(t) \frac{\cosh(k_{pq}(z+h))}{\cosh(k_{pq}h)} e^{ik_{xp}x + ik_{yq}y}, \quad (5)$$

where $k_{xp} = p \frac{2\pi}{L_x}$, $k_{yq} = q \frac{2\pi}{L_y}$ and $k_{pq} = |(k_{xp}, k_{yq})|$. L_x and L_y are the lengths of the horizontal computational domain. The modal amplitudes $A_{pq}^{(m)}(t)$ can be solved by a Fast Fourier Transform. Then, the vertical velocity on the free surface, $\phi_z(x, y, \eta)$, is computed from the z -derivative of Eqn. (5), and ϕ and η can be time-stepped based on Eqns. (2) and (3).

A 4th-order Runge-Kutta method is adopted for time stepping. The sawtooth instabilities in HOS are controlled by a second-order Savitzky-Golay filter in the physical space and a low-pass filter in the Fourier space. According to Xiao (2013), the low-pass filter Λ has the form of an exponential function,

$$\Lambda(k_x, k_y | k_{xc}, k_{yc}) = \exp \left\{ \sqrt{\left(\frac{k_x}{k_{xc}}\right)^2 + \left(\frac{k_y}{k_{yc}}\right)^2}^{-n} \right\}, \quad (6)$$

where $n = 30$, the wavenumber vector of each component is $\mathbf{k} = (k_x, k_y)$. k_{xc} and k_{yc} are the cut-off wavenumber in the x and y directions, respectively. Following the *half-rule* (West *et al.*, 1987), $k_{xc} = k_{xmax}/2$ and $k_{yc} = k_{ymax}/2$ where k_{xmax} and k_{ymax} are the maximum wavenumbers of the Fourier space in the directions of x and y , respectively.

We apply a dynamic correction to model the ship through the applied surface pressure p in Eqn. (3). The dynamic correction strategy was initially proposed by Lindberg *et al.* (2013). The desired hull shape is described by $\eta_s(x, y, t)$, and the static pressure of the ship is defined as

$$p_s(x, y, t) = -\rho g \eta_s(x, y, t) = \rho g T f(x, t) q(y, t), \quad (7)$$

where

$$f(x, t) = \begin{cases} \cos^2 \left[\frac{\pi(|x-x^*(t)| - \frac{1}{2}\alpha L)}{(1-\alpha)L} \right] & \frac{1}{2}\alpha L \leq |x-x^*(t)| \leq \frac{1}{2}L \\ 1 & |x-x^*(t)| \leq \frac{1}{2}\alpha L \end{cases}, \quad (8)$$

$$q(y, t) = \begin{cases} \cos^2 \left[\frac{\pi(|y-y^*(t)| - \frac{1}{2}\beta B)}{(1-\beta)B} \right] & \frac{1}{2}\beta B \leq |y-y^*(t)| \leq \frac{1}{2}B \\ 1 & |y-y^*(t)| \leq \frac{1}{2}\beta B \end{cases}. \quad (9)$$

The coordinates of the center of the water plane are (x^*, y^*) , and they are a function of the time t . The length, width and draft of the ship are denoted by L , B and T , respectively. α and β are coefficients which control the shape of the wetted hull surface in the x and y directions, respectively. Note that η_s and p_s are zero outside the ship region defined by $-L/2 \leq (x-x^*) \leq L/2$ and $-B/2 \leq (y-y^*) \leq B/2$.

The problem is initialized with $\eta = \eta_s$ and $p = p_s$. At subsequent time steps, we apply a dynamic correction about the ship pressure given by

$$p = -\rho g \eta_s + \rho g (\eta - \eta_s) - \frac{\rho}{2} [\nabla \phi^S \cdot \nabla \phi^S - \phi_z^2 (1 + \nabla \eta \cdot \nabla \eta)] + \rho U(t) \frac{\partial \phi^S}{\partial x} \quad (10)$$

$$= -2\rho g \eta_s + \rho g \eta - \frac{\rho}{2} [\nabla \phi^S \cdot \nabla \phi^S - \phi_z^2 (1 + \nabla \eta \cdot \nabla \eta)] + \rho U(t) \frac{\partial \phi^S}{\partial x}. \quad (11)$$

The first term in Eqn. (10) is the static pressure of the hull and the rest of the terms are the dynamic correction which forces the surface potential towards the desired steady-state convective result at speed U . In the computation, the ship pressure p expressed by Eqn. (11) is applied in the free-surface boundary condition, i.e. Eqn. (3).

3 Results and discussion

In this paper, some of the test cases in the experiments conducted by Ertekin *et al.* (1984) are chosen for the numerical simulation. In the experiment, a model of a Series 60 with block coefficient $C_B = 0.8$ travels along the centerline of the channel. The width of the channel is $W = 1.22$ m. The length, width and draft of the ship

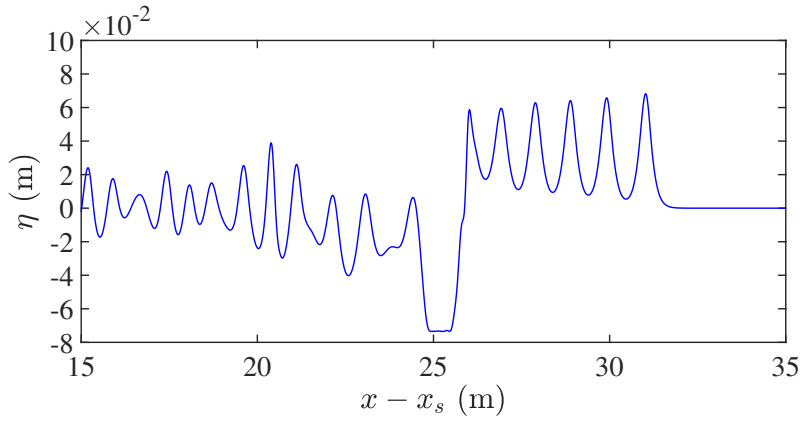


Figure 1: The surface elevation η on the centerline of the channel at $t = 22.73$ s in the test case with $Fr=1.0$. The water depth is $h = 0.125$ m. x_s is the initial position of the center of water plane in the x -direction. The numerical results are computed by HOS ($M = 3$). The region of ship bottom is in the range of $24.91 \leq (x - x_s) \leq 25.47$ m. The nonlinear upstream waves are in the range of $26.49 \leq (x - x_s) \leq 32.02$ m.

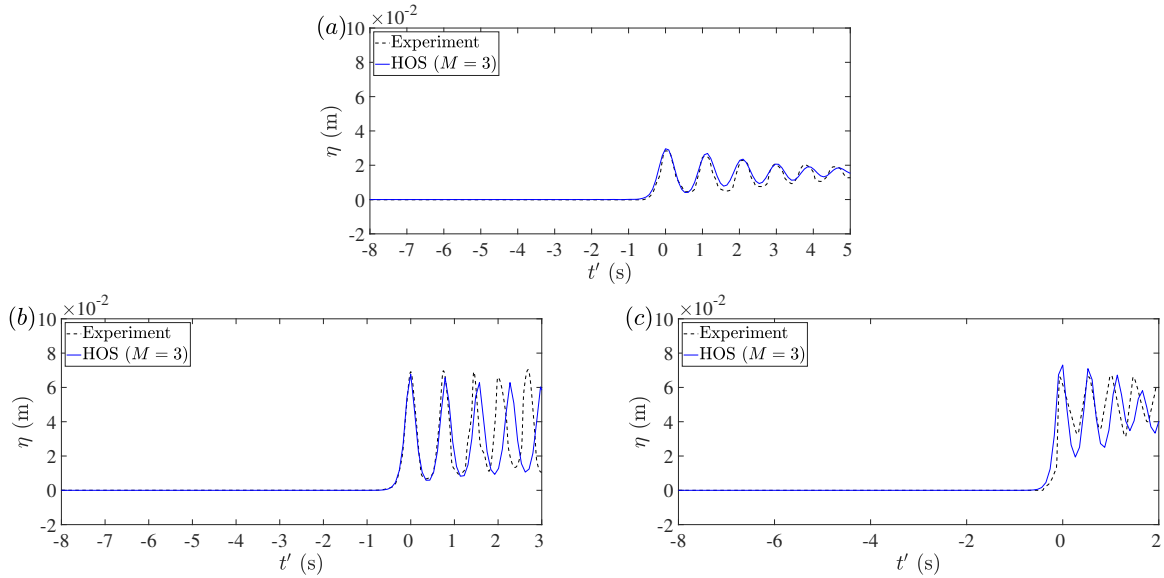


Figure 2: Wave records from the gauge placed along the centerline of the channel. The blue solid line denotes the numerical results obtained using HOS ($M = 3$). The black dashed line denotes the experimental records. (a) $Fr=0.8$, (b) $Fr=1.0$, (c) $Fr=1.1$.

model are $L = 1.524$ m, $B = 0.234$ m and $T = 0.075$ m, respectively. The model ship starts impulsively. Various Froude numbers Fr and different water depths h are chosen in the test cases. In the numerical simulation, the nonlinear order of the HOS model is set as $M = 3$. The length and width of the computational domain are $L_x = 122.88$ m and $L_y = 1.22$ m, respectively. The number of nodes in the direction of L_x and L_y are $N_x = 8192$ and $N_y = 128$, respectively.

Firstly, we study three test cases in which the water depth is $h = 0.125$ m. Different Froude numbers are adopted, i.e. $Fr=0.8$, 1.0 and 1.1 . Figure 1 shows the surface elevation on the centerline of the channel at $t = 22.73$ s in the test case with $Fr=1.0$. x_s is the initial position of the center of water plane in the x -direction. The region of ship bottom is at $24.91 \leq (x - x_s) \leq 25.47$ m, where the surface elevation is nearly a straight line. The absolute value of the surface elevation in the region of ship bottom stays around 0.075 m, which corresponds to the value of ship draft T . The correlation between the surface elevation in the ship region and the ship form is attributed to the dynamic correction of ship pressure. The nonlinear upstream waves are shown in the range of $26.49 \leq (x - x_s) \leq 32.02$ m. The first wave at around $(x - x_s) = 31.02$ m is the main wave with a peak of 0.068 m. The amplitude of the four small waves propagating behind the main wave shows a decreasing trend. Furthermore, the mean level of the upstream waves is above zero.

To measure the formation of upstream waves, a gauge was placed along the centerline of the channel in the experiment. Correspondingly, in the numerical simulation, a numerical wave gauge is set at the same position as the experiment. Therefore, the reliability of the numerical results can be ensured by comparing the records from the numerical wave gauge and the gauge in the experiment. The results of the three test cases in which $Fr=0.8$, 1.0 and 1.1 , respectively, are illustrated in Fig. 2. The peak of the main wave is placed at $t' = 0$ in the

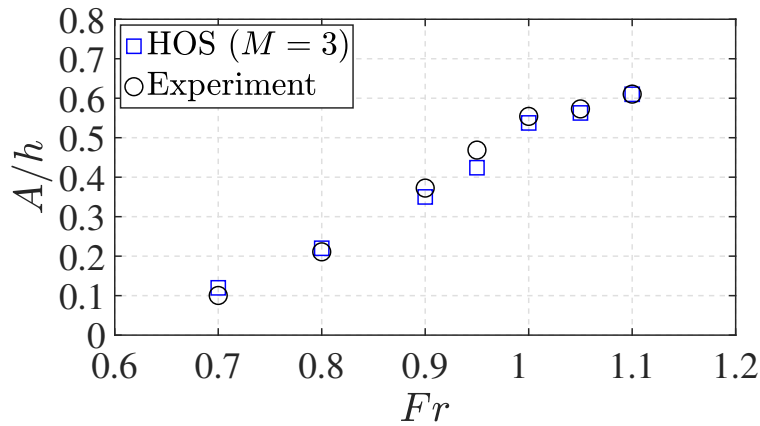


Figure 3: The variation of the non-dimensional amplitude A/h of the main upstream wave with the Froude number Fr . The water depth is $h = 0.15$ m. The Froude number Fr is set as 0.7, 0.8, 0.9, 0.95, 1.0, 1.05 and 1.1, respectively. The blue square represents the numerical results computed by HOS ($M = 3$). The black circle denotes the experimental records.

plots. In each of the three test cases, the records from the numerical wave gauge correspond reasonably well to the experimental data, which gives confidence in the accuracy of the HOS model. Moreover, the decrease of the amplitude of the small waves propagating behind the main wave is more significant in the test case with $Fr = 0.8$ than that in the test cases with $Fr = 1.0$ and 1.1. The mean level of the upstream waves increase with Fr .

Next, the water depth h is set as 0.15 m. The upstream waves in the test cases in which Fr varies from 0.7 to 1.1 are investigated. The amplitude of the main wave recorded by the gauge on the centerline of the channel is made non-dimensional with respect to the water depth, i.e. A/h . The variation of A/h with Fr is illustrated in Fig. 3. The numerical results compare well with the experimental records. The amplitude of the main wave increases with the Froude number; however, the increasing trend is suppressed for $Fr \geq 1$. In the supercritical conditions, the amplitude of the main wave is approximately 5-6 times the water depth.

4 Conclusion

A high-order spectral (HOS) model is adopted to simulate the evolution of upstream waves generated by a ship traveling at near-critical speeds ($Fr \sim 1$). The traveling ship is modeled by a moving pressure distribution with dynamic correction. Some experiments with different Froude numbers Fr and water depths h in Ertekin *et al.* (1984) are chosen for the model validation. Because of the dynamic correction strategy of the ship pressure, the surface elevation in the ship region obtained using HOS ($M = 3$) corresponds well to the ship form. The forms of upstream waves computed by HOS ($M = 3$) are comparable to those recorded in the experiments, which gives confidence in the accuracy of the present numerical model.

References

- DOMMERMUTH, D. G. & YUE, D. K. P. 1987 A high-order spectral method for the study of nonlinear gravity waves. *J. Fluid Mech.* **184**, 267–288.
- ERTEKIN, R. C., WEBSTER, W. C. & WEHAUSEN, J. V. 1984 Ship-generated solitons. In *Proc. 15th Symp. Nav. Hydrodyn. Hamburg*.
- ERTEKIN, R. C., WEBSTER, W. C. & WEHAUSEN, J. V. 1986 Waves caused by a moving disturbance in a shallow channel of finite width. *J. Fluid Mech.* **169**, 275–292.
- GRUE, J. 2022 On the generation process of upstream waves by a pressure distribution at critical speed. In *37th International Workshop on Water Waves and Floating Bodies, Giardini Naxos*.
- LI, Y. & SCLAVOUNOS, P. D. 2002 Three-dimensional nonlinear solitary waves in shallow water generated by an advancing disturbance. *J. Fluid Mech.* **470** (1), 383–410.
- LINDBERG, O., GLIMBERG, S. L., BINGHAM, H. B., ENGSIG-KARUP, A. P. & SCHJELDAHL, P. J. 2013 Towards real time simulation of ship-ship interaction - part II: Double body flow linearization and GPU implementation. In *28th International Workshop on Water Waves and Floating Bodies, Marseille, France*.
- SHI, F., MALEJ, M., SMITH, J. M. & KIRBY, J. T. 2018 Breaking of ship bores in a Boussinesq-type ship-wake model. *Coastal Eng.* **132**, 1–12.
- WEST, B., BRUECKNER, K., JANDA, R. S., MILDER, D. M. & MILTON, R. L. 1987 A new numerical method for surface hydrodynamics. *J. Geophys. Res.* **92**, 11803–11824.
- WU, T. Y. 1987 Generation of upstream advancing solitons by moving disturbances. *J. Fluid Mech.* **184** (1), 75–99.
- WU, T. Y. & WU, D. M. 1982 Three-dimensional nonlinear long waves due to moving surface pressure. In *Proc. 14th Symp. Nav. Hydrodyn. Ann Arbor, Michigan, USA*.
- XIAO, W. 2013 Study of directional ocean wavefield evolution and rogue wave occurrence using large-scale phase-resolved nonlinear simulations. PhD thesis, Massachusetts Institute of Technology, Cambridge, MA.